Published in final edited form as:
Endocr Relat Cancer. 2008 September ; 15(3): 787–799. doi:10.1677/ERC-08-0079.

Re-expression *of ABI3BP* Suppresses Thyroid Tumor Growth by Promoting Senescence and Inhibiting Invasion

Flavia R. M. Latini[1], **Jefferson P. Hemerly**[1], **Gisele Oler**[1], **Gregory J. Riggins**[2], and **Janete M. Cerutti**[1]

[1] Genetic Bases of Thyroid Tumors Laboratory, Division of Genetics, Department of Morphology and Genetics; Federal University of São Paulo, SP, Brazil

[2] Department of Neurosurgery, Johns Hopkins University School of Medicine, Baltimore, MD, USA

Abstract

Loss of *ABI* gene family member 3 binding protein (*ABI3BP*) expression may be functionally involved in the pathogenesis of cancer. Previous reports have indicated a loss of expression in lung cancer and a presumed role in inducing cellular senescence. We show here that *ABI3BP* expression is significantly decreased in most malignant thyroid tumors of all types. To better understand *ABI3BP's* role we created a model by re-expressing *ABI3BP* in two thyroid cancer cell lines. Re-expression of *ABI3BP* in thyroid cells resulted in a decrease in transforming activity, cell growth, cell viability, migration, invasion and tumor growth in nude mice. *ABI3BP* re-expression appears to trigger cellular senescence through the *p21* pathway. Additionally, *ABI3BP* induced formation of HP1γ-positive senescence-associated heterochromatin foci (SAHF) and accumulation of senescence-associated β-galactosidase. The combination of a decrease in cell growth, invasion and other effects upon *ABI3BP* re-expression *in vitro* helps explain the large reduction in tumor growth we observed in nude mice. Together, our data provides evidence that the loss of *ABI3BP* expression could play a functional role in thyroid tumorigenesis. Activation of *ABI3BP* or its pathway may represent a possible basis for targeted therapy of certain cancers.

Keywords

TARSH; *ABI3BP*; thyroid carcinoma; senescence; invasion and migration

Introduction

We have previously identified biomarkers that distinguish malignant follicular thyroid carcinoma (FTC) from benign follicular thyroid adenoma (FTA) with high sensitivity and specificity (Cerutti J. M. *et al.*, 2004). These four genes also help distinguish malignant tumors in a wide range of thyroid tumors (Cerutti J. M. *et al.*, 2006). The expression studies, performed originally to locate clinical markers, also revealed genes expressed in non-malignant tissues (normal thyroid and FTA), but not expressed or expressed at lower levels in the malignant FTC. One of these genes, *ABI3BP*, formerly named *TARSH*, was of particular interest because it was expressed in nearly all FTAs and normal thyroid samples, with consistent down-regulation in all FTCs (Cerutti J. M. *et al.*, 2004).

Requests for reprints should be addressed to: Janete M. Cerutti, Ph. D. Rua Pedro de Toledo 669, 11° andar. Federal University of São Paulo, 04039-032, São Paulo, SP, Brazil, Phone: +55-11-5081-5233 fax: +55-11-5084-5231, E-mail: j.cerutti@unifesp.br.

Conflict of interest: The authors declare that they have no affiliations that would constitute a financial conflict of interest relating to the subject matter of this study.

Although the biology of *ABI3BP* (*ABI3* binding protein) is largely unknown, it has been suggested that ABI3BP interacts with a SH3 domain in ABI3 (Abl-interactor member 3) (Matsuda *et al.*, 2001). ABI3, along with the Abl-interactors E3B1/Abi2/Argbp1, belong to the family of cytoplasmic molecular adaptors containing SH3 that interact with Abl-family tyrosine kinases. Although speculative, it seems that members of Abl-interactors family might negatively regulate cell growth and transformation by suppressing certain tyrosine kinase-mediated signaling in mammalian cells (Ichigotani *et al.*, 2002a). Overexpression of these family members was associated with inhibited cell proliferation, reduced transforming potential, and suppression of motility and metastasis dissemination (Ichigotani *et al.*, 2002a, Ichigotani *et al.*, 2002b). These findings suggest that Abl-interactors may act as tumor suppressor molecules. Therefore, if ABI3BP binds to the Abl-interactor ABI3, it is predicted to result in inhibited cell growth. Circumstantial evidence consistent with a function for *ABI3BP* that suppresses cell proliferation is the report that its expression is greatly reduced in lung cancers and other primary tumors (Terauchi *et al.*, 2006).

In the present study, we sought to determine if loss of *ABI3BP* expression play a role in thyroid tumorigenesis. We expanded our analysis and investigated the expression of *ABI3BP* in a larger series of thyroid tumors which includes, in addition to a larger number of FTAs and FTCs, Hürthle cell adenomas, Hürthle cell carcinomas, papillary thyroid carcinomas and normal thyroids. *ABI3BP* is lost in most of malignant lesions while it is expressed in a large number of benign lesions and normal thyroid tissues. We next explored functionally the effects of *ABI3BP* re-expression into two thyroid carcinoma cell lines in which *ABI3BP* expression was lost. Additionally, we suggest a possible pathway in which *ABI3BP* is involved. Finally, we show that *ABI3BP* re-expression has an effect on subcutaneous tumors of thyroid origin grown in nude mice.

Materials and Methods

Tissue samples

A total of 79 thyroid tissue specimens obtained from patients undergoing thyroid surgery for thyroid disease at Hospital São Paulo, Federal University of São Paulo, Brazil were used for this study. Samples were frozen immediately after surgical biopsy and stored at −80°C and included 36 benign thyroid lesions (21 follicular thyroid adenomas and 15 Hürthle cell adenomas), 36 malignant thyroid tumors (17 follicular thyroid carcinomas, 6 Hürthle cell carcinomas, and 13 papillary thyroid carcinomas), and 7 normal thyroid tissues. All tissue samples were obtained with informed consent according to established Human Studies Protocols at Federal University of São Paulo. The study of patient materials was conducted according to the principles expressed in the Declaration of Helsinki.

Cell lines

A follicular (WRO) and an undifferentiated (ARO) thyroid carcinoma cell lines were used in this study (generous gifts of Dr. Alfredo Fusco, University Federico II, Naples, Italy). WRO and ARO were grown in DMEM (Invitrogen Corp., Carlsbad, CA) supplemented with 10% FBS (Invitrogen), 100 units/mL of penicillin and 100 μg/mL streptomycin in a humidified incubator containing 5% at CO_2 37ºC. ARO and WRO cell lines are known to have a number of specific genetic abnormalities including *RAS*, *p53* and *BRAF* mutation (Kimura *et al.*, 2003, Ouyang *et al.*, 2002).

RNA extraction, cDNA synthesis and quantitative PCR (qPCR) of *ABI3BP* in human tissues

Total RNA and cDNA synthesis were performed as previously described (Cerutti J. M. *et al.*, 2004). An aliquot of cDNA was used in a 15μL PCR reaction containing 1X TaqMan universal PCR master mix, 10μmol of each specific primer and FAM-labeled probe for the target gene

(*ABI3BP*) or VIC-labeled probe for reference gene (*RS8*) (TaqMan®Gene Assays on Demand; Applied Biosystems, Foster City, CA). Quantitative PCR reactions (qPCR) were performed in triplicate and the threshold cycle (Ct), obtained using Applied Biosystems software (Applied Biosystems), was averaged (SD ≤1). Gene expression was calculated as described (Cerutti J. M. *et al.*, 2004).

Plasmids constructs

To obtain the full-length human *ABI3BP* coding sequence, cDNA was synthesized from RNA isolated from normal thyroid tissue and used as template for PCR amplification using the sense 5′TAAATGCAGCTCCAGGGTTG3′ and antisense 5′CTCCTCCGCAAAGCTATTCA3′ primers. PCR product was purified and cloned into the mammalian expression vector pcDNA3.1 using a directional TOPO expression kit (Invitrogen) according to manufacturer's recommendations. This DNA construct was sequenced to confirm the sense orientation as described (Guimaraes *et al.*, 2006).

Stable expression in thyroid carcinoma cell lines

To establish cell lines expressing *ABI3BP*, 10μg of DNA construct was transfected into 5×10^6 WRO and ARO cells by electroporation using a Gene Pulser II (Bio-Rad Laboratories Inc., Hercules, CA). ARO and WRO cells transfected with pcDNA3.1 vector were used as controls. Clones were isolated after 3 weeks of selection with G418 (800μg/mL). At least six G418-resistant clones from each transfection were isolated, expanded, maintained on G418 (400μg/mL), and tested for *ABI3BP* expression by qPCR. To this end, total RNA extracted from each clone was used for cDNA synthesis as described (Cerutti J. M. *et al.*, 2004). An aliquot of cDNA was used in 20μL PCR reaction containing SYBR Green PCR Master Mix (Applied Biosystems) and 200 nM of each primer for *ABI3BP* or reference gene (ribosomal protein *S8*). Primer sequences for *ABI3BP* and reference gene were as follows: *ABI3BP* sense 5′ TTGCCAAGTCACTGTCCCAAT3′ and antisense 5′ GTGGCTGGACAGATTTGAAAAAT3′, yielding a product of 93bp; S8 sense 5′ TGAAAGGAAAAAGAATGCCAAAA3′ and antisense 5′ CACTGTCCCGGCCTTGAA 3′, yielding a product of 96bp. qPCR was performed in triplicate and the threshold cycle (Ct), obtained using Applied Biosystems software (Applied Biosystems), was averaged (SD ≤1). Gene expression was normalized to the average of *S8*. Relative expression was calculated as described (Cerutti J. M. *et al.*, 2004). For each cell line, two independently isolated clones that stably express *ABI3BP* and two pcDNA3.1 clones were used for further *in vitro* and *in vivo* experiments.

Focus formation assay

Five × 10^6 WRO cells were transfected with 10μg of either pcDNA3.1 or DNA construct coding *ABI3BP* as described above. After 3 weeks of selection with G418 (800μg/mL), WRO cells were fixed in 10% acetic acid and 10% of methanol, stained with 1% crystal violet, and colonies were counted (Iervolino *et al.*, 2006).

MTT assay

ARO cells were analyzed with the 3-(4,5-dimethylthiazol-2-yl)-2,5-diphenyl-tetrazolium bromide (MTT) assay. In brief, 2×10^4 ARO cells were seeded in 35-mm plates on day 0. Cell growth was measured daily from day 1 to 5 by adding 0.5 mg/mL of MTT (Sigma-Aldrich, St. Louis, MO) in medium at 37°C for 3 hours. The medium was removed and the purple formazan crystals were dissolved in acid isopropanol at room temperature for 10 minutes. The spectrophotometric absorbance was measured at 560 nm.

Cell viability assay

ARO cells (2×10^4) were seeded in 35-mm plates. Cells were mixed with Guava ViaCount Reagent and allowed to stain for 10 minutes (Guava Technologies, Hayward, CA). The Guava System differentiates viable from nonviable cells by detecting fluorescent signals from two fluorescent DNA-binding dyes: one membrane-permeable dye stains all nucleated cells while the second dye enters cells with compromised membrane integrity, i.e., nonviable cells. Viable cells were quantified using a Guava Personal Analyzer (PCA) flow cytometer (Guava Technologies) following the manufacturer's specifications. Experiments were performed in quintuplicate.

Quantification of apoptotic cells by annexin-V labeling

ARO cells (2×10^4) were seeded in 35-mm plates. For detection of apoptosis, the cells were double-stained with annexin V and nexin 7-AAD according to the manufacturer's recommendations (Guava Nexin method; Guava Technologies). Cell-associated fluorescence was analyzed by the Guava PCA flow cytometer (Guava Technologies). Results are expressed as the percentage of apoptotic positive cells. Both early apoptotic (annexin V-positive) and late apoptotic (annexin V- and 7 AAD-positive) cells were included in the analysis. Experiments were performed in quintuplicate.

Cellular senescence

Senescence-associated (SA) β-gal staining was performed as described (Severino *et al.*, 2000). Briefly, ARO cells (2×10^4) were seeded in 35-mm plates. On referred days, cells were washed twice with PBS, fixed for 15 minutes and stained with 1 mg/mL 5-bromo-4-chloro-3-inolyl- b-D-galactosidase (X-gal) in buffer (dimethylformamide, 40 mM citric acid/sodium phosphate pH 6.0, 5 mM potassium ferrocyanide, 5 mM potassium ferricyanide, 150 mM NaCl and 2 mM $MgCl_2$). Cells were incubated at 37°C in 5% CO_2 for 18 hours and washed twice with PBS. Cells were examined using a light microscope and counted in 5 optical fields (100X). Data represents mean of an experiment performed in quintuplicate.

Senescence-associated heterochromatic foci (SAHF)

Another feature of senescence cells is formation of senescence-associated heterochromatin foci (SAHF) (Collado *et al.*, 2005, Narita *et al.*, 2003). Formation of such structures coincides with the recruitment of protein complexes containing the heterochromatin 1 binding protein γ (HP1γ). The HP1γ expression was analyzed using immunofluorescence. Cells were plated at a density of 1.7×10^2 cells per well in an 8-well glass slide (Nalge Nunc International, Rochester, NY). At day 5, cells were washed with PBS and fixed in methanol. Plates were blocked using 20% normal goat serum in PBS/Tween-20 and incubated for at least 16 hours at 4ºC with HP1γ primary antibody (1/500; MAB3450; Chemicon, Temecula, CA). Cells were counterstained using DAPI.

Expression of *p21*, *E2F1*, *MMP-1* and *Ki67* by qPCR

Expression analysis was performed at days 3 and 5. Total RNA isolation and cDNA synthesis were performed as described (Cerutti J. M. *et al.*, 2007). An aliquot of cDNA was used in 20μL PCR reaction containing SYBR Green PCR Master Mix (Applied Biosystems) and 200 nM of each primer for target gene or reference gene (ribosomal protein *S8*). Primer sequences were as follows: *p21* sense 5′TGGAGACTCTCAGGGTCGAAA3′ and antisense 5′ GGCTTCCTCTTGGAGAAGATCA3′, yielding a product of 90bp; *Ki67* sense 5′ GTCGACGGTCCCCACTTTC3′ and antisense 5′GACACAACAGGAAGCTGGATACG3′, yielding a product of 92bp; *E2F1* sense 5′TTGAGGGCATCCAGCTCATT3′ and antisense 5′ CCTGGGTCAACCCCTCAAG3′, yielding a product of 105bp; and *MMP-1* sense 5′

TGTGGCTCAGTTTGTCCTCACT3′ and antisense 5′GGCAAATCTGGCGTGTAATTTT3′ yielding a product of 90bp.

Protein extraction and western blotting analysis

Protein extraction and western blotting analysis were performed according to standard procedures. Briefly, total protein was isolated from clones expressing *ABI3BP* and vector-transfected clones using an extraction buffer containing 50 mM Tris HCl (pH 7.4), 100 mmol/L NaCl, 50 mM NaF, 1 mM NaVO4, 0.5 % NP-40 and complete protease inhibitor cocktail (Roche, Mannheim, Germany). The whole cell extract was clarified by centrifugation at 10,000 × g. Protein concentration was estimated with a Bradford assay (Sigma-Aldrich). About 50μg of protein was loaded into pre-cast 4–12% SDS-NuPage Bis-Tris Gel (Invitrogen). After transfer, the membrane was blocked and incubated for at least 16 hours at 4°C with anti-phospho-AKT (pAKT; cat# 9271; dilution 1:400) or anti-phospho-ERK (pERK; cat# 9102; dilution 1:1000) purchased from Cell Signaling (Beverly, MA) or anti-α-tubulin (cat#T9026; dilution 1:1000) purchased from Sigma-Aldrich. After incubation with anti-rabbit or anti-mouse peroxidase conjugated secondary antibodies (DAKO, Glostrup, Denmark, dilution 1:5000) proteins were detected using Super Signal West Pico Chemiluminescent Substrate purchased from Pierce (Rockford, IL).

Cell cycle analysis

ARO cells (2×10^5) were seeded in 35-mm dishes. After synchronization of the cells by serum starvation for 24 hours, cells were replaced with DMEM medium supplemented with 10% FBS for 24 hours. Cells were fixed in 70% ethanol for 1 hour, labeled with Guava Cell Cycle Assay reagent and analyzed using Guava PCA flow cytometer (Guava Technologies) according to manufacturer's recommendation. Experiments were performed in quintuplicate.

Anchorage-independent growth

Anchorage-independent growth was assessed by a double-layer soft agar assay. Initially, 60-mm dishes were layered with 0.5% agar and 1X complete medium. Subsequently, ARO cells (1.5×10^4) were suspended in 1X complete medium and 0.35% agar and seeded in triplicate over a bottom layer of solidified agar. The dishes were incubated at 37°C in 5% CO_2. After 3 weeks, colonies greater than 20μm in diameter were counted. Colony formation rate was calculated as percentage of total seeded cells. Two independent experiments were performed.

Nude mouse xenograft model

Four to five week old male athymic nude (*nu*/*nu*) mice were maintained according to the guidelines of the Division of Animal Resources at the Federal University of São Paulo. ARO stable cell clones were suspended in sterile PBS to 2×10^6/200μL and injected subcutaneously into the flank of individual nude mice. Mice were then monitored biweekly during three weeks. If a tumor was present, volume was calculated by the rotational ellipsoid formula: $V = A \times B^2/2$ (A = axial diameter; B = rotational diameter). Tumor tissues were collected and were either embedded in paraffin for conventional histology or stored at −80°C. Additionally, we also extracted RNA from formed tumors, performed cDNA synthesis and tested by qPCR *ABI3BP*, *p21* and *MMP-1* expressions as described above.

Matrigel invasion assay

Cell invasion was analyzed using BioCoat Matrigel Invasion Chamber according to the manufacturer's recommendation (Becton Dickinson, Bedford, MA). FBS was used as chemoattractant. WRO cell clones were added to the invasion or control chamber at a density of 2.5×10^4 and, after 24 hours, cells remaining above the insert membrane were removed by gentle scraping with a sterile cotton swab. Cells that had invaded through the Matrigel to the

bottom of the insert were fixed, stained in rapid panoptic LB (Laborclin, Brazil) and mounted. Cells were examined using a light microscope and counted in 3 optical fields (100X). All of the experimental and control groups were done in triplicate. The percentage of invasion cells was determined as the mean of cells invading through Matrigel insert membrane/mean of cell migrating through control insert membrane X100.

Migration assay

To assess cell migration, WRO stable cell clones were suspended in 10mL of DMEM supplemented with 10% FBS, seeded onto 0.75% agar base coated plates prepared in DMEM and cultured until spheroids were formed. At least 12 spheroids of similar diameter were placed in the middle of uncoated 24-well plates. The area covered by cells spreading out from the spheroid was measured at the beginning of the experiment and daily for an observation period of 6 days. The areas of spheroids were calculated as described (Vajkoczy *et al.*, 2006).

Statistical analysis

The qPCR values were log transformed and submitted to Student's *t* test (unpaired). *In vitro* results were log transformed and submitted to Student's *t* test (paired). *In vivo* results were submitted to Wilcoxon test. Were declared significant the results with $P < 0.05$.

Results

ABI3BP is under-expressed in malignant thyroid lesions

Among the genes we previously analyzed as underexpressed in follicular thyroid carcinomas, *ABI3BP* stood out because of its consistent loss in malignant follicular tumors (Cerutti J. M. *et al.*, 2004). We extended our previous analysis by also including Hürthle cell carcinomas, papillary thyroid carcinomas and the benign Hürthle cell adenomas in our assay. As demonstrated by qPCR, *ABI3BP* expression was either reduced or absent in most thyroid carcinomas (follicular thyroid carcinomas, Hürthle cell carcinomas and papillary thyroid carcinomas), when compared to normal thyroid and most of benign lesions (follicular thyroid adenomas and Hürthle cell adenomas; P=0.0001; Fig 1*A*). Surprisingly *ABI3BP* was up regulated in few adenomas, compared to normal samples. Although samples were not matched to one another, it may suggest that these pre-malignant lesions may express *ABI3BP* as a mechanism to prevent proliferation of cells at risk for neoplastic transformation. Additionally, *ABI3BP* was consistently under expressed in thyroid carcinomas. Therefore, we hypothesized that *ABI3BP* is functionally involved in suppressing either thyroid tumor growth or tumor progression.

Re-expression of *ABI3BP* in thyroid carcinoma cell lines

To explore *ABI3BP's* potential pathogenic role, we generated an *in vitro* thyroid cancer model. As previously demonstrated, ARO thyroid carcinoma cell line do not express *ABI3BP*. WRO express *ABI3BP* at very low levels (Cerutti J. M. *et al.*, 2004). A construct expressing *ABI3BP* and an empty vector were transfected into both cell lines. Several stable clones were obtained from each transfected cell line and qPCR was used to assess levels of *ABI3BP*. Two representative clones from each group were chosen for our studies. As shown in Fig. 1*B*, the qPCR data demonstrated that *ABI3BP* transcripts were induced about 2000-fold in ARO-transfected with a construct encoding *ABI3BP*. WRO-transfected with a construct encoding *ABI3BP* had an average 2-fold increase in *ABI3BP* (Fig 1*B*). This fold-induction was obtained when *ABI3BP* expression was normalized to vector-transfected clones (endogenous expression). Importantly, when the clones re-expressing *ABI3BP* were normalized to the expression observed in normal thyroids, the relative expression observed in ARO-*ABI3BP* transfected cells was similar to the biological range observed in most normal thyroid and

adenomas. The WRO-*ABI3BP* transfected cells had expression similar to that observed in the few adenomas with greater *ABI3BP* expression (data not shown). Based on the ability to obtain physiologic levels of *ABI3BP* in ARO cells, and that the ARO line before transfection has a high tumorigenic potential (Cerutti J. *et al.*, 1996), ARO clones were used in most of the experiments in this work. WRO clones were chosen for migration and invasion assays and foci formation, because ARO does not aggregate into spheroids, does not migrate through Matrigel within 24 hours and it was difficult to measure foci formation as ARO has a high growth rate.

Expression of *ABI3BP* reduces colony formation in thyroid cancer cells

To see if *ABI3BP* could inhibit foci formation, the vector only or the expression construct encoding *ABI3BP* was transfected into the WRO cell line. When WRO was transfected with a vector containing wild-type human *ABI3BP*, the number of colonies was significantly reduced (0.8 foci/μg of plasmid DNA) when compared to the number observed with control vector (32.7 foci/μg of plasmid DNA; $P< 0.05$; Fig. 1*C*). This significant reduction in the number of colonies suggests that *ABI3BP* reduces the malignant potential of the WRO cells.

Expression of *ABI3BP* inhibits cell growth

To determine if *ABI3BP* re-expression decreases proliferation, the stably transfected clones were compared to controls by a MTT assay. As showed in Fig. 2*A*, *ABI3BP* was able to significantly suppress the growth of ARO cells in comparison with the cells transfected with empty vector ($P<0.05$).

Effect of *ABI3BP* on cell viability and apoptosis

To ascertain if re-expression of *ABI3BP* would decrease thyroid cancer cell's viability, the Guava ViaCount Reagent was used. The Guava ViaCount reagent contains two fluorescent dyes, one cell permeable and one impermeable to cells with an intact plasma membrane. As determined by ViaCount, re-expression of *ABI3BP* led to a lower percentage of viable cells ($P<0.05$; Fig. 2*B*). This finding suggests that re-expression of *ABI3BP* might induce apoptosis. To quantify the apoptotic rate of ARO cells expressing *ABI3BP*, we analyzed annexin-V binding using a Guava Nexin kit, which reveals phosphatidylserine externalization in apoptotic cells. Re-expression of *ABI3BP* led to a moderate increase of apoptosis (Fig. 2*C*), which suggest that another mechanism may also be involved in inhibition of cell growth and decrease of cell viability. Since *ABI3BP* was previously associated with senescence process (Uekawa *et al.*, 2005) and it was previously suggested that senescence may interfere with cell membrane integrity (Xin *et al.*, 2003), a percentage of nonviable cells observed may represent senescent cells.

ABI3BP expression induces senescence in ARO cells

Senescent cells stain positive for SA-β-gal and a distinct heterochromatic structure designed as senescence associated heterochromatin formation (SAHF). We first observed that SA-β-Gal positive cells, indicated by blue staining, were increased when *ABI3BP* is re-expressed (Fig. 2*D, E*). Secondly, immunofluorescence of HP1γ showed an expression pattern concentrated in DNA foci of cells expressing *ABI3BP* compared to controls which suggested that the re-expression of *ABI3BP* was associated with the nuclear changes that occur during senescence. Conversely in vector-transfected cells, the staining for HP1γ gave a weak signal and it was disperse through the nucleoplasm (Fig. 2*F*).

ABI3BP reduces expression of the proliferation marker *Ki67* in ARO cells

As aforementioned, *ABI3BP* significantly suppress the growth of ARO cells. In order to measure cell proliferation, beyond the MTT test, expression levels of the proliferation marker

Ki67 were tested at days 3 and 5. As measured by *Ki67* expression, a lower proliferation rate was observed in ARO re-expressing *ABI3BP* when compared to control cells (Fig. 3*A*).

ABI3BP induces senescence markers in ARO cells

We have shown that ARO cells undergo senescence process following *ABI3BP* re-expression, although the underlie mechanism is still unclear. Several genes/pathways were associated with senescence process and elucidation of the pathway that control senescence is complex. To start to build a model, we here investigate the potential role of a number of previously identified senescence markers (*p21, E2F1* and *MMP-1*) (Brown *et al.*, 1997, Collado & Serrano, 2006, Collado *et al.*, 2000, Narita *et al.*, 2003, Park *et al.*, 2006). We used qPCR to quantify mRNA levels of tested markers at days 3 and 5, a time that cells re-expressing *ABI3BP* became positive for SA-β-Gal staining, have decreased expression of proliferation marker and nuclei were positive for HP1γ. At day 5, a time in which senescence process was more evident, *p21* mRNA levels were 3-fold increased in ARO cells following *ABI3BP* re-expression ($P<0.05$; Fig. 3*A*). The expression of *MMP-1* was significantly increased at days 3 and 5 ($P<0.001$; Fig. 3*A*). On the other hand, *E2F1* mRNA levels were reduced in ARO expressing *ABI3BP* (Fig. 3*A*). Of note, E2F1-responsive genes were stably repressed in senescent cells. It was demonstrated that HP1γ mediate SAHF formation and *E2F* gene silencing occurs during senescence (Narita *et al.*, 2003).

ABI3BP re-expression alters AKT and ERK phosphorilation

The effect of *ABI3BP* re-expression was further substantiated by investigation of AKT and ERK signaling pathways. The re-expression of *ABI3BP* resulted in a slight decreased ERK phosphorylation mainly at day 5 compared with vector-transfected cells. Meanwhile, a significant increase in AKT phosphorylation was observed at day 5 (Fig. 3*B*).

ABI3BP causes a decrease in cells in S and G_2/M

Cell cycle distribution was analyzed by flow cytometry. G_0/G_1 arrest occurred in ARO cells expressing *ABI3BP* as indicated by an increase in the percentage number of cells at this phase (Fig. 4*A*). Although cell cycle was not investigated at day 5, when senescence phenotype was marked observed, the cell proliferation marker *Ki67* was down-regulated and the cell cycle inhibitor *p21* was up-regulated at day 5 (Fig. 3*A*). These findings suggest an important growth arrest at day 5.

ABI3BP affects anchorage-independent cell growth

We evaluated whether the expression of *ABI3BP* had an effect on the *in vitro* transformed phenotype using soft-agar colony-forming assay. Soft-agar growth of *ABI3BP* transfected cells was reduced when compared to those of control vector-transfected ARO (Fig. 4*B*).

ABI3BP reduces tumor growth in nude mice

Although the anchorage-independent growth was not reduced at significant levels, other *in vitro* results encouraged us to investigate whether *ABI3BP* had potential in reducing tumor formation in nude mice. ARO cells expressing *ABI3BP* did not form tumors in nude mice (n=2) or formed a very small tumor ($0.11 \pm 0.6 cm^3$; n=4). In contrast, control mice had extensive tumors (3.62 ± 2.84 cm^3; n=8; Fig. 4*C*). Interestingly, in one control mouse, a marked tumor vascularization was observed. Therefore, a significant decrease in tumor formation, represented as mean of tumor volume, is demonstrated in mice with cells expressing *ABI3BP* when compared with controls ($P=0.027$; Fig. 4*D*). When presented, an aliquot of tumor was stored at −80ºC and a fraction was processed for routine histology and immunohistochemical analysis. H&E staining revealed the presence of tumors within the flank of 100% of controls. Neither lung nor lymph node metastases were found in any mice.

Senescence markers on tumor growth in nude mice

Since we observed an increased expression of senescence markers in cells re-expressing *ABI3BP*, they were also investigated in tumor samples that were taken from tumors growing on the flanks of nude mice. The expression of *p21*, *MMP-1* and *ABI3BP* was assayed by qPCR. A higher expression of *p21* and *MMP-1* were detected in tumors formed after injection of cells expressing *ABI3BP* compared to tumors formed upon injection of control cells (Fig. 4*E*). These findings corroborate with our *in vitro* analysis and suggest that *ABI3BP* induces senescence-like growth arrest through modulation of the *p21* pathway.

ABI3BP inhibited invasion and migration of WRO cells

Given these *in vivo* and *in vitro* findings, we sought to determine invasion and migration potential of cells expressing *ABI3BP*. Cellular invasiveness was quantified using BioCoat Matrigel Invasion Chamber. WRO cells expressing *ABI3BP* significantly attenuated cellular invasiveness (30.92%) when compared with cells transfected with empty vector (62.86%; Fig. 5*A, B*). The migration ability was demonstrated by a spheroid growth assay. We observed the reduction in spheroid area in *ABI3BP*-expressing cells. A more significant effect on migration was observed in WRO cells expressing *ABI3BP* at day 6 compared with control (Fig. 5*C*).

Discussion

Our previous work suggested a consistent loss of *ABI3BP* expression in malignant follicular thyroid carcinoma (Cerutti J. M. *et al.*, 2004). In this study, we expanded our analysis of follicular thyroid tumors and also included other thyroid tumors subtypes. *ABI3BP* expression was either reduced or absent not just in FTCs, but in most malignant lesions and thyroid carcinoma cell lines compared with benign lesions and normal thyroid tissues. Therefore, loss of *ABI3BP* expression is not restricted to a specific malignant histological subtype. Recently, others have showed that *ABI3BP* expression was significantly decreased in several tumor types when compared to the expression in corresponding non-neoplastic tissue specimens (Terauchi *et al.*, 2006). This expression pattern hints that *ABI3BP* might play a role in maintaining a normal phenotype in several types of cancer.

We next sought to determine if *ABI3BP* was functionally involved in thyroid malignancy. We tested the effects of re-expression of *ABI3BP* on thyroid carcinoma cells *in vitro* and *in vivo*. Several lines of evidence from this research support the hypothesis that *ABI3BP* reduces tumor growth and progression.

We first demonstrated that the ectopic expression of *ABI3BP* inhibits foci formation and reduces cellular proliferation and viability. Furthermore, the results show that *ABI3BP* markedly affected tumor growth *in vivo*. Since growth inhibitory effects may be caused by the re-establishment of programmed cell death, we next investigated the role of *ABI3BP* in apoptosis. Although forced *ABI3BP* expression increased apoptosis, the small percentage of apoptotic cells could not fully explain the larger reduction on cell proliferation and viability. Another mechanism that controls cell proliferation and restricts tumor growth is cellular senescence.

Since senescent cells may remain viable, one could argue that senescence could not be the mechanism by which *ABI3BP* reduces proliferation and tumor growth. However, it is important to note that oxidative stress, observed during senescence process, may interfere with cell membrane integrity (Xin *et al.*, 2003). Therefore, a proportion of non-viable cells observed upon *ABI3BP* re-expression may represent senescent cells that have lost membrane integrity and were detected because they were permeable to the dye.

There are additional evidences suggesting that *ABI3BP* could potentially induce senescence. Several groups detected the occurrence of senescence in premalignant tumor whereas cells in malignant tumors are unable to trigger senescence (Chen *et al.*, 2005, Collado *et al.*, 2005, Michaloglou *et al.*, 2005). Therefore, they conclude that senescence worked as a barrier to prevent progression of cells that are at risk for tumorigenic transformation (Chen *et al.*, 2005, Collado & Serrano, 2006).

Given that *ABI3BP* expression is lost in thyroid malignancies and that others implicate the murine homologue (*mABI3BP*) in stress-induced senescence in mouse embryonic fibroblasts (Uekawa *et al.*, 2005), we investigated whether senescence could be an additional growth inhibitory mechanism for *ABI3BP* expression.

We infer from our findings that *ABI3BP* induces cellular senescence, suggesting that senescence might be the preferential mechanism associated with growth inhibitory effect observed in cells expressing *ABI3BP*. It is an important aspect because prevention of tumor progression can be done either by inducing apoptosis or senescence (Collado & Serrano, 2006). Since cellular senescence is an important tumor suppression process, the characterization of genetic pathways to senescence is needed.

It has been observed that various forms of stress including DNA-damaging agents, oncogenic activation, oxidative stress and inadequate culture conditions induce a state that is indistinguishable from replicative senescence which was called premature senescence or stress-induced senescence (Campisi, 2001, Lowe *et al.*, 2004, Serrano & Blasco, 2001). Although the molecular mechanism underlying the senescence process remains poorly understood, recent studies have provided mechanistic insights into the senescence process. There is no doubt that constitutively active mutants of *RAS*/*RAF* provoke premature senescence *in vivo* and *in vitro*, additional alteration may be necessary to maintain an irreversible state of growth arrest. Investigation of the signaling pathways showed that inactivation of one of the effectors of the p53 or RB pathways is required to bypass senescence (Itahana *et al.*, 2001, Mason *et al.*, 2004, Michaloglou *et al.*, 2005, Narita *et al.*, 2003). How *p53* and *RB* induce senescence is not completely understood and may be cell type and context-dependent. As suggest by recent report, RB contributes to senescence by promoting senesce-associated heterochromatin foci (SAHF) and by silencing E2F targets genes (Itahana *et al.*, 2001, Narita *et al.*, 2003).

Although reliable, molecular markers for the senescent state are still missing, some characteristics such as senescence-associated β-galactosidase (SA-β-gal) activity, *Ki67* down-regulation, expression of cell cycle inhibitors such as *p21* and chromatin remodeling have proven useful as indicators of cellular senescence (Braig & Schmitt, 2006). Therefore, the investigation of these senescence-associated phenotypes will help to clarify the role of *ABI3BP*.

ARO cell line exhibits a number of specific genetic changes that may be a mechanism of tumor cells to evade senescence, including *BRAF* V600E and *p53* mutation (Fagin *et al.*, 1993, Kimura *et al.*, 2003). Interestingly, when the ARO cell line was stably transfected with wild-type *p53*, effects similar to those seen when we re-expressed *ABI3BP* were observed (Nagayama *et al.*, 2000). Whether the re-expression of *ABI3BP* induces senescence by restoring p53 pathway and/or interfering with RAS/RAF/MAPK/ERK pathway may lead to a better and novel understanding on how *ABI3BP* induces senescence.

A rational approach would be investigating the level of expression of *p21*, which is downstream of p53 and appears to be essential for induction of senescence (Itahana *et al.*, 2001). We here demonstrated that *p21* mRNA was up-regulated following *ABI3BP* re-expression compared to control cells, in both *in vitro* and *in vivo* analysis. Although the mechanism that underlies the

p21 induction is unknow, ectopic expression of *ABI3BP* induces changes in gene expression that resemble the gene expression changes that occur in senescent cell.

Since several other proteins have been implicated in this complex process, a question that immediately comes to our minds is: what other proteins may be involved in senescence process induced by *ABI3BP*?

It was demonstrated that constitutive activation of AKT promotes senescence-like growth arrest via p21-dependent pathway (Miyauchi *et al.*, 2004). Recently, it was demonstrated that AKT-dependent inactivation of FOXO3a induced many senescence phenotypes such as SA-β-Gal staining and up-regulation of *p53* and *p21* (Kyoung Kim *et al.*, 2005). Additionally, it has been suggested that AKT participates in the regulation of both p53-dependent and p53-independent *p21* expression (Mitsuuchi *et al.*, 2000). A markedly increased expression of pAKT was observed in ARO cells re-expressing *ABI3BP*, mainly at day 5 when most of senescence-associated phenotype was observed, such as SA-β-Gal staining, senescence-associated heterochromatin foci formation (SAHF), *p21* overexpression, *Ki67* down-regulation and *in vitro* and *in vivo* growth inhibition.

E2F1 is among the growth regulatory genes that are repressed during senescence (Dimri *et al.*, 1994), although this is controversial (Dimri *et al.*, 2000, Park *et al.*, 2006). The contradictory activities of *E2F1* may be due to cell context. We here demonstrated that *E2F1* was underexpressed in cells re-expressing *ABI3BP* when compared to controls. This result corroborates with previous findings in which lower *E2F1* expression was associated with a favorable prognosis in breast cancer (Vuaroqueaux *et al.*, 2007) and a higher *E2F1* expression was found in papillary and anaplastic thyroid cancers (Onda *et al.*, 2004).

Regarding the RAS/RAF/MAPK/ERK pathways, it has been suggested that RAF-induced senescence appears to have no obvious requirement for either p53 or p21 (Zhu *et al.*, 1998). Although we have found a slight decrease in pERK, our findings suggest that it may occur through independent mechanism.

However, the senescence phenotype is not only mainly characterized by irreversible arrest of cell division and gene expression changes aforementioned. Senescent cells also express genes that have no obvious direct role in cell proliferation but are associated with remodeling. For example, cells may develop a constitutive matrix-degrading phenotype by secreting large amounts of matrix metalloproteinases such *MMP-1* (interstitial collagenase) (Collado & Serrano, 2006, Linskens *et al.*, 1995). We here found an increased expression of *MMP-1* in ARO cells re-expressing *ABI3BP* compared to control cells in both *in vivo* and *in vitro*.

Furthermore, besides its role in growth suppression and the determination of some components of the signaling pathways through which *ABI3BP* induces senescence, we here investigated the role of *ABI3BP* in invasion and migration. In this report, we show that *ABI3BP* significantly reduces spheroid growth and the percentage of invading cells in Matrigel. These findings, together with the *in vivo* results, strongly suggest that *ABI3BP* impairs migration and invasive ability of thyroid carcinoma cell line.

It is worth noting that *ABI3BP* was described to be an *ABI3-binding protein*, as it was isolated from a human placenta cDNA library using the SH3 domain of human ABI3, formerly named NESH (Matsuda *et al.*, 2001). ABI3 is an adaptor protein that, through the SH3 domain, interacts with Abl-family tyrosine kinases and suppresses the transforming activity in mammalian cells. It was also suggested that the loss of *ABI3* expression could be involved in the mechanism of cell motility and metastasis (Ichigotani *et al.*, 2002b). One can postulate that ABI3BP may interact with ABI3 or other abl-interactor to regulate actin cytoskeleton (Hirao

et al., 2006, Ichigotani *et al.*, 2002b). However, the mechanism by which *ABI3BP* inhibits migration and invasion remains to be understood.

The mechanism by which *ABI3BP* is under expressed is unknown. PCR amplification and karyotype analysis did not detect loss of heterozygosis at 3q12 where *ABI3BP* is located (data not shown). Methylation analysis of the region could find an epigenetic alteration responsible for its expression loss, although using the CpG plot program, we did not find CpG islands in the promoter region of *ABI3BP* (www.ebi.ac.uk/emboss/cpgplot). Another likely explanation is that an activated tyrosine kinase could lead to down-regulation of *ABI3BP*, as usually occurs with Abl-interactors (Ichigotani *et al.*, 2002b).

Interestingly, we previous identified five *isoforms* of *ABI3BP* in thyroid tissues, most of them expressed in normal thyroid tissues and not expressed in malignant lesions (Guimaraes *et al.*, 2006). One specific isoform, an insertion of 265 bp in intron 24, which generates a premature stop codon, was found only in FTC. These findings suggest that alternative splicing could be a mechanism responsible for *ABI3BP* loss of expression. Interestingly, alternative splicing of *ABI3BP* was also described in murine (Uekawa *et al.*, 2005).

Based on our findings we suggest that *ABI3BP* inhibits cell growth, reduces cell viability, promotes senescence, and decreases migration and invasion *in vitro*. All these features are consistent with the fact that *ABI3BP* behaves to reduce tumor growth when re-expressed in thyroid cancer cells.

Of note, many of chemotherapeutic agents used in clinical are assumed to exert their anti-tumor effect through induction of apoptosis. Since *ABI3BP* may act to suppress growth in thyroid and possibly other tumor types, understanding its molecular mechanism of suppression is of great interest. The possibility is raised if increasing *ABI3BP* expression levels through pharmacological or other means may be useful to inhibit malignant growth and invasion. Chemotherapy-induced premature senescence could represent an alternative approach to treat tumors that are resistant to conventional therapies.

Acknowledgments

This project was supported by NIH Grant CA113461, and the São Paulo State Research Foundation (FAPESP) from grants 04/15288-0 and 05/60330-8. JMC is investigator of the Brazilian Research Council (CNPq), FRML and GO are scholars from FAPESP and GJR is the recipient of the Irving J. Sherman M.D. Research Professorship.

References

Braig M, Schmitt CA. Oncogene-induced senescence: putting the brakes on tumor development. Cancer Res 2006;66:2881–2884. [PubMed: 16540631]

Brown JP, Wei W, Sedivy JM. Bypass of senescence after disruption of p21CIP1/WAF1 gene in normal diploid human fibroblasts. Science 1997;277:831–834. [PubMed: 9242615]

Campisi J. Cellular senescence as a tumor-suppressor mechanism. Trends Cell Biol 2001;11:S27–31. [PubMed: 11684439]

Cerutti J, Trapasso F, Battaglia C, Zhang L, Martelli ML, Visconti R, Berlingieri MT, Fagin JA, Santoro M, Fusco A. Block of c-myc expression by antisense oligonucleotides inhibits proliferation of human thyroid carcinoma cell lines. Clin Cancer Res 1996;2:119–126. [PubMed: 9816098]

Cerutti JM, Oler G, Michaluart P Jr, Delcelo R, Beaty RM, Shoemaker J, Riggins GJ. Molecular profiling of matched samples identifies biomarkers of papillary thyroid carcinoma lymph node metastasis. Cancer Res 2007;67:7885–7892. [PubMed: 17699795]

Cerutti JM, Delcelo R, Amadei MJ, Nakabashi C, Maciel RM, Peterson B, Shoemaker J, Riggins GJ. A preoperative diagnostic test that distinguishes benign from malignant thyroid carcinoma based on gene expression. J Clin Invest 2004;113:1234–1242. [PubMed: 15085203]

Cerutti JM, Latini FR, Nakabashi C, Delcelo R, Andrade VP, Amadei MJ, Maciel RM, Hojaij FC, Hollis D, Shoemaker J, et al. Diagnosis of suspicious thyroid nodules using four protein biomarkers. Clin Cancer Res 2006;12:3311–3318. [PubMed: 16740752]

Chen Z, Trotman LC, Shaffer D, Lin HK, Dotan ZA, Niki M, Koutcher JA, Scher HI, Ludwig T, Gerald W, et al. Crucial role of p53-dependent cellular senescence in suppression of Pten-deficient tumorigenesis. Nature 2005;436:725–730. [PubMed: 16079851]

Collado M, Serrano M. The power and the promise of oncogene-induced senescence markers. Nat Rev Cancer 2006;6:472–476. [PubMed: 16723993]

Collado M, Medema RH, Garcia-Cao I, Dubuisson ML, Barradas M, Glassford J, Rivas C, Burgering BM, Serrano M, Lam EW. Inhibition of the phosphoinositide 3-kinase pathway induces a senescence-like arrest mediated by p27Kip1. J Biol Chem 2000;275:21960–21968. [PubMed: 10791951]

Collado M, Gil J, Efeyan A, Guerra C, Schuhmacher AJ, Barradas M, Benguria A, Zaballos A, Flores JM, Barbacid M, et al. Tumour biology: senescence in premalignant tumours. Nature 2005;436:642. [PubMed: 16079833]

Dimri GP, Hara E, Campisi J. Regulation of two E2F-related genes in presenescent and senescent human fibroblasts. J Biol Chem 1994;269:16180–16186. [PubMed: 8206919]

Dimri GP, Itahana K, Acosta M, Campisi J. Regulation of a senescence checkpoint response by the E2F1 transcription factor and p14(ARF) tumor suppressor. Mol Cell Biol 2000;20:273–285. [PubMed: 10594030]

Fagin JA, Matsuo K, Karmakar A, Chen DL, Tang SH, Koeffler HP. High prevalence of mutations of the p53 gene in poorly differentiated human thyroid carcinomas. J Clin Invest 1993;91:179–184. [PubMed: 8423216]

Guimaraes GS, Latini FR, Camacho CP, Maciel RM, Dias-Neto E, Cerutti JM. Identification of candidates for tumor-specific alternative splicing in the thyroid. Genes Chromosomes Cancer 2006;45:540–553. [PubMed: 16493598]

Hirao N, Sato S, Gotoh T, Maruoka M, Suzuki J, Matsuda S, Shishido T, Tani K. NESH (Abi-3) is present in the Abi/WAVE complex but does not promote c-Abl-mediated phosphorylation. FEBS Lett 2006;580:6464–6470. [PubMed: 17101133]

Ichigotani Y, Fujii K, Hamaguchi M, Matsuda S. In search of a function for the E3B1/Abi2/Argbp1/NESH family (Review). Int J Mol Med 2002a;9:591–595. [PubMed: 12011975]

Ichigotani Y, Yokozaki S, Fukuda Y, Hamaguchi M, Matsuda S. Forced expression of NESH suppresses motility and metastatic dissemination of malignant cells. Cancer Res 2002b;62:2215–2219. [PubMed: 11956071]

Iervolino A, Iuliano R, Trapasso F, Viglietto G, Melillo RM, Carlomagno F, Santoro M, Fusco A. The receptor-type protein tyrosine phosphatase J antagonizes the biochemical and biological effects of RET-derived oncoproteins. Cancer Res 2006;66:6280–6287. [PubMed: 16778204]

Itahana K, Dimri G, Campisi J. Regulation of cellular senescence by p53. Eur J Biochem 2001;268:2784–2791. [PubMed: 11358493]

Kimura ET, Nikiforova MN, Zhu Z, Knauf JA, Nikiforov YE, Fagin JA. High prevalence of BRAF mutations in thyroid cancer: genetic evidence for constitutive activation of the RET/PTC-RAS-BRAF signaling pathway in papillary thyroid carcinoma. Cancer Res 2003;63:1454–1457. [PubMed: 12670889]

Kyoung Kim H, Kyoung Kim Y, Song IH, Baek SH, Lee SR, Hye Kim J, Kim JR. Down-regulation of a forkhead transcription factor, FOXO3a, accelerates cellular senescence in human dermal fibroblasts. J Gerontol A Biol Sci Med Sci 2005;60:4–9. [PubMed: 15741276]

Linskens MH, Feng J, Andrews WH, Enlow BE, Saati SM, Tonkin LA, Funk WD, Villeponteau B. Cataloging altered gene expression in young and senescent cells using enhanced differential display. Nucleic Acids Res 1995;23:3244–3251. [PubMed: 7667101]

Lowe SW, Cepero E, Evan G. Intrinsic tumour suppression. Nature 2004;432:307–315. [PubMed: 15549092]

Mason DX, Jackson TJ, Lin AW. Molecular signature of oncogenic ras-induced senescence. Oncogene 2004;23:9238–9246. [PubMed: 15489886]

Matsuda S, Iriyama C, Yokozaki S, Ichigotani Y, Shirafuji N, Yamaki K, Hayakawa T, Hamaguchi M. Cloning and sequencing of a novel human gene that encodes a putative target protein of Nesh-SH3. J Hum Genet 2001;46:483–486. [PubMed: 11501947]

Michaloglou C, Vredeveld LC, Soengas MS, Denoyelle C, Kuilman T, van der Horst CM, Majoor DM, Shay JW, Mooi WJ, Peeper DS. BRAFE600-associated senescence-like cell cycle arrest of human naevi. Nature 2005;436:720–724. [PubMed: 16079850]

Mitsuuchi Y, Johnson SW, Selvakumaran M, Williams SJ, Hamilton TC, Testa JR. The phosphatidylinositol 3-kinase/AKT signal transduction pathway plays a critical role in the expression of p21WAF1/CIP1/SDI1 induced by cisplatin and paclitaxel. Cancer Res 2000;60:5390–5394. [PubMed: 11034077]

Miyauchi H, Minamino T, Tateno K, Kunieda T, Toko H, Komuro I. Akt negatively regulates the in vitro lifespan of human endothelial cells via a p53/p21-dependent pathway. Embo J 2004;23:212–220. [PubMed: 14713953]

Nagayama Y, Yokoi H, Takeda K, Hasegawa M, Nishihara E, Namba H, Yamashita S, Niwa M. Adenovirus-mediated tumor suppressor p53 gene therapy for anaplastic thyroid carcinoma in vitro and in vivo. J Clin Endocrinol Metab 2000;85:4081–4086. [PubMed: 11095436]

Narita M, Nunez S, Heard E, Lin AW, Hearn SA, Spector DL, Hannon GJ, Lowe SW. Rb-mediated heterochromatin formation and silencing of E2F target genes during cellular senescence. Cell 2003;113:703–716. [PubMed: 12809602]

Onda M, Nagai H, Yoshida A, Miyamoto S, Asaka S, Akaishi J, Takatsu K, Nagahama M, Ito K, Shimizu K, et al. Up-regulation of transcriptional factor E2F1 in papillary and anaplastic thyroid cancers. J Hum Genet 2004;49:312–318. [PubMed: 15118916]

Ouyang B, Knauf JA, Ain K, Nacev B, Fagin JA. Mechanisms of aneuploidy in thyroid cancer cell lines and tissues: evidence for mitotic checkpoint dysfunction without mutations in BUB1 and BUBR1. Clin Endocrinol (Oxf) 2002;56:341–350. [PubMed: 11940046]

Park C, Lee I, Kang WK. E2F-1 is a critical modulator of cellular senescence in human cancer. Int J Mol Med 2006;17:715–720. [PubMed: 16596252]

Serrano M, Blasco MA. Putting the stress on senescence. Curr Opin Cell Biol 2001;13:748–753. [PubMed: 11698192]

Severino J, Allen RG, Balin S, Balin A, Cristofalo VJ. Is beta-galactosidase staining a marker of senescence in vitro and in vivo? . Exp Cell Res 2000;257:162–171. [PubMed: 10854064]

Terauchi K, Shimada J, Uekawa N, Yaoi T, Maruyama M, Fushiki S. Cancer-associated loss of TARSH gene expression in human primary lung cancer. J Cancer Res Clin Oncol 2006;132:28–34. [PubMed: 16205947]

Uekawa N, Terauchi K, Nishikimi A, Shimada J, Maruyama M. Expression of TARSH gene in MEFs senescence and its potential implication in human lung cancer. Biochem Biophys Res Commun 2005;329:1031–1038. [PubMed: 15752759]

Vajkoczy P, Knyazev P, Kunkel A, Capelle HH, Behrndt S, von Tengg-Kobligk H, Kiessling F, Eichelsbacher U, Essig M, Read TA, et al. Dominant-negative inhibition of the Axl receptor tyrosine kinase suppresses brain tumor cell growth and invasion and prolongs survival. Proc Natl Acad Sci U S A 2006;103:5799–5804. [PubMed: 16585512]

Vuaroqueaux V, Urban P, Labuhn M, Delorenzi M, Wirapati P, Benz CC, Flury R, Dieterich H, Spyratos F, Eppenberger U, et al. Low E2F1 transcript levels are a strong determinant of favorable breast cancer outcome. Breast Cancer Res 2007;9:R33. [PubMed: 17535433]

Xin MG, Zhang J, Block ER, Patel JM. Senescence-enhanced oxidative stress is associated with deficiency of mitochondrial cytochrome c oxidase in vascular endothelial cells. Mech Ageing Dev 2003;124:911–919. [PubMed: 14499496]

Zhu J, Woods D, McMahon M, Bishop JM. Senescence of human fibroblasts induced by oncogenic Raf. Genes Dev 1998;12:2997–3007. [PubMed: 9765202]

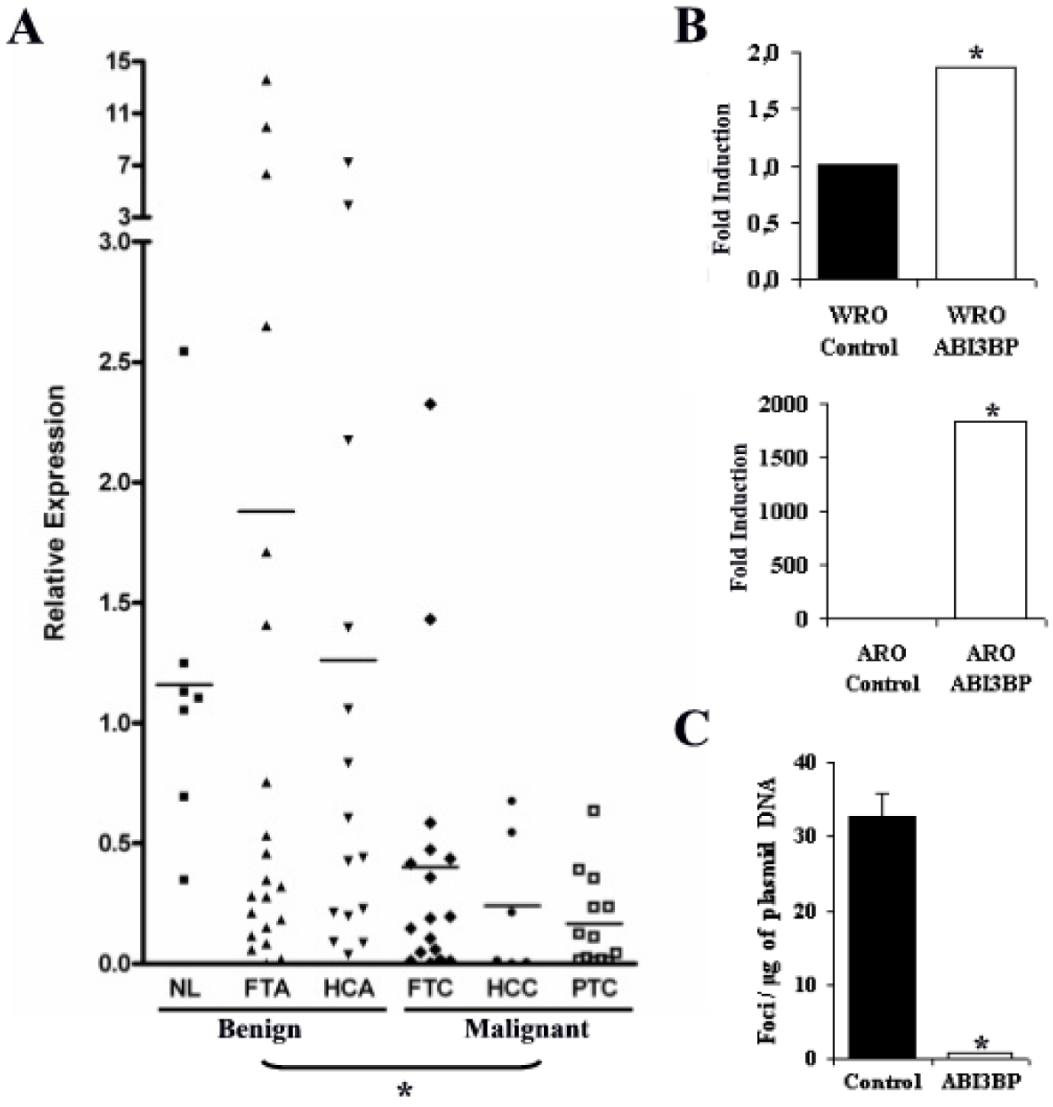

Figure 1.

Relative expression levels of *ABI3BP* in thyroid tumors and cell lines and its ability to decrease foci formation. In *A*, symbols correspond to the relative expression values for *ABI3BP* in normal thyroid tissues (NT; n=7■), follicular thyroid adenomas (FTA; n=21▲), Hürthle cell adenomas (HCA; n=15▼;), follicular thyroid carcinomas (FTC; n=17◆), Hürthle cell carcinomas (HCC; n=6•) and papillary thyroid carcinomas (PTC; n=13□). The qPCR values were log transformed before application of statistical test (*P*=0.0001). In *B*, qPCR analysis of stably transfected clones selected for the *in vitro* and *in vivo* experiments. The analysis demonstrated that *ABI3BP* expression was induced about 2000-fold in ARO-transfected with a construct encoding *ABI3BP* when normalized to vector-transfected cells. WRO cells had an average 2-fold increased basal-level expression when transfected with a construct encoding *ABI3BP*. In *C*, transforming potential of a construct encoding *ABI3BP* in WRO cell line compared to a pcDNA3.1 empty vector control. *ABI3BP* decreased dramatically the transformation ability of WRO cells (0.8 foci/µg of plasmid DNA) compare to control (32.7 foci/µg of plasmid DNA). Black bar corresponds to WRO transfected with control clones and

white bar to the cells transected with *ABI3BP* expression vector. The data represents the mean ± SD of the experiment performed in triplicate.

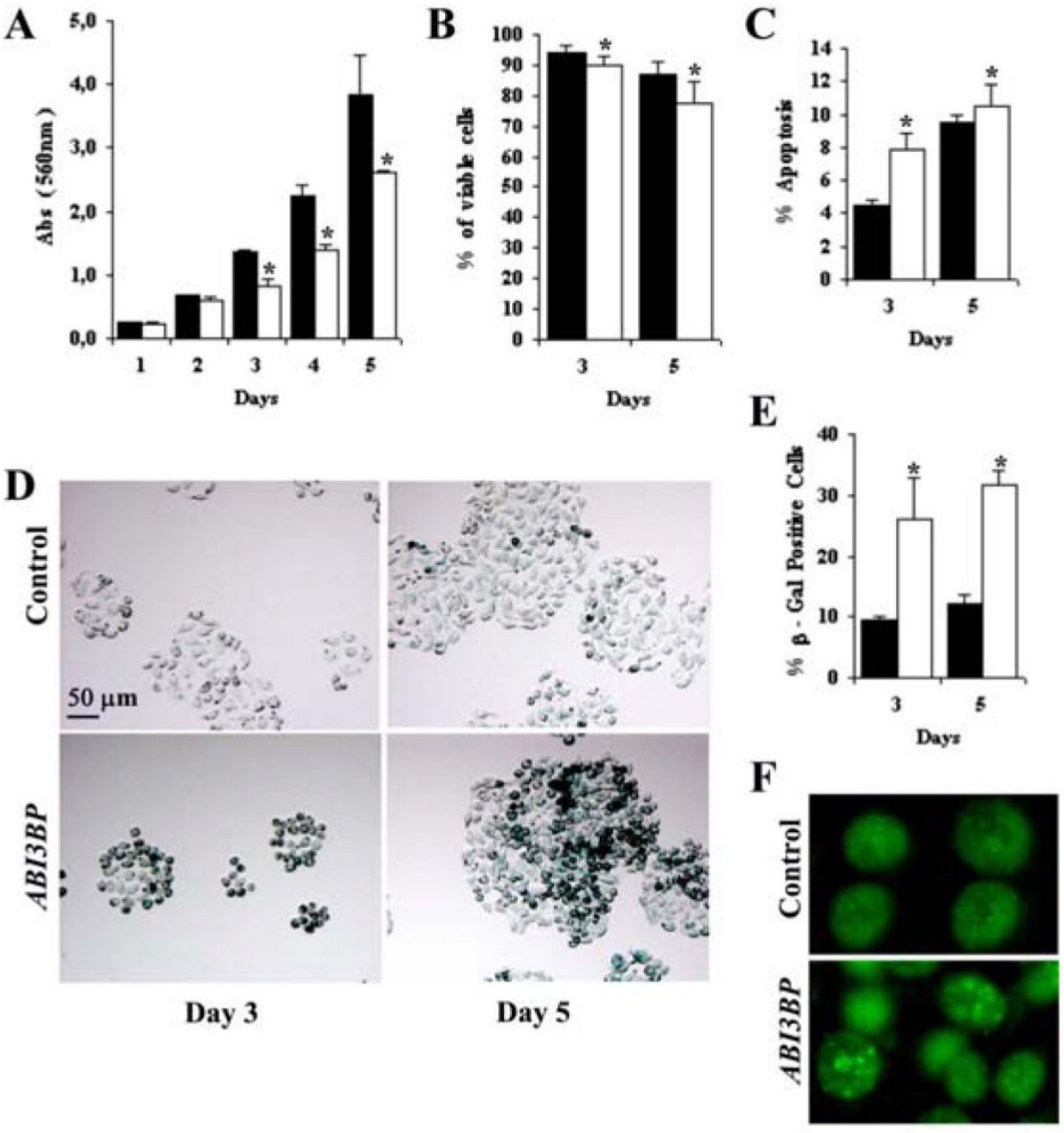

Figure 2.

Effect of *ABI3BP* re-expression on proliferation, viability, apoptosis and senescence in ARO thyroid carcinoma cells. Black bars correspond to control clones (n=2) and white bars correspond to *ABI3BP* expressing clones (n=2). In *A*, is shown the effect of *ABI3BP* expression on proliferation suppression in the ARO cell line, detected by an MTT assay. The data represents the mean ± SD of absorbance at 560 nm of at least two experiments performed in triplicates on each of five days. In *B*, the mean of percentage ± SD of viable cells shows a decrease with *ABI3BP* expression. The decrease with *ABI3BP* was 5% at day 3 and 10% at day 5. In *C*, Guava Nexin assay is represented by the mean ± SD of the percentage of apoptotic cells from quintuplicate. The percentage of apoptotic cells was higher in cells expressing

ABI3BP compared to control cells (3% at day 3 and 1% at day 5). In *D*, representative results illustrate increased senescence-associated β-galactosidase (SA-β-gal) staining with *ABI3BP* expression on days 3 and 5. In *E*, the SA- β-gal staining is represented by the mean ± SD of the percentage of β-galactosidase positive cells from quintuplicate experiments. The percentage of β-galactosidase positive cells was higher in ARO cells expressing *ABI3BP*. In *F*, representative results of immunofluorescence for HP1γ, which demonstrated that enforced expression of was sufficient to induce SAHF.

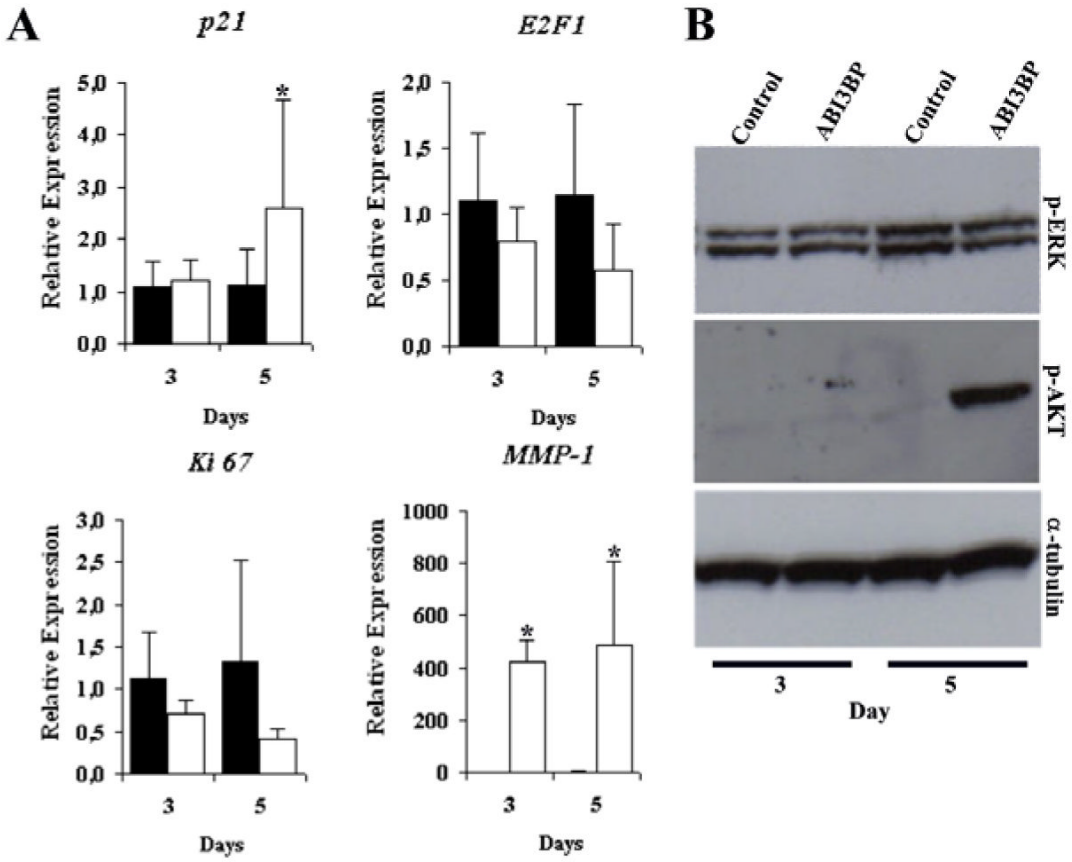

Figure 3.

Expression of proliferation and senescence-associated markers following re-expression of *ABI3BP*. Black bars correspond to control clones (n=2) and white bars correspond to *ABI3BP* expressing clones (n=2). In *A*, graphs show mean ± SD of *Ki67*, *p21*, *E2F1* and *MMP-1* relative expression levels on days 3 and 5. A decrease of *Ki67* and *E2F1* and an increase *p21* and *MMP-1* mRNA was observed following *ABI3BP* re-expression, mainly at day 5 when senescence was more evident. In *B*, whole-cell lysates (50μg) of ARO *ABI3BP* re-expressing versus control cells were analyzed for the phospho-ERK (pERK) and phospho-AKT (pAKT). *ABI3BP* re-expression was associated with slight decreased pERK at days 3 and 5. A significant increase of pAKT was observed at day five. As a protein loading control, we analyzed α-tubulin.

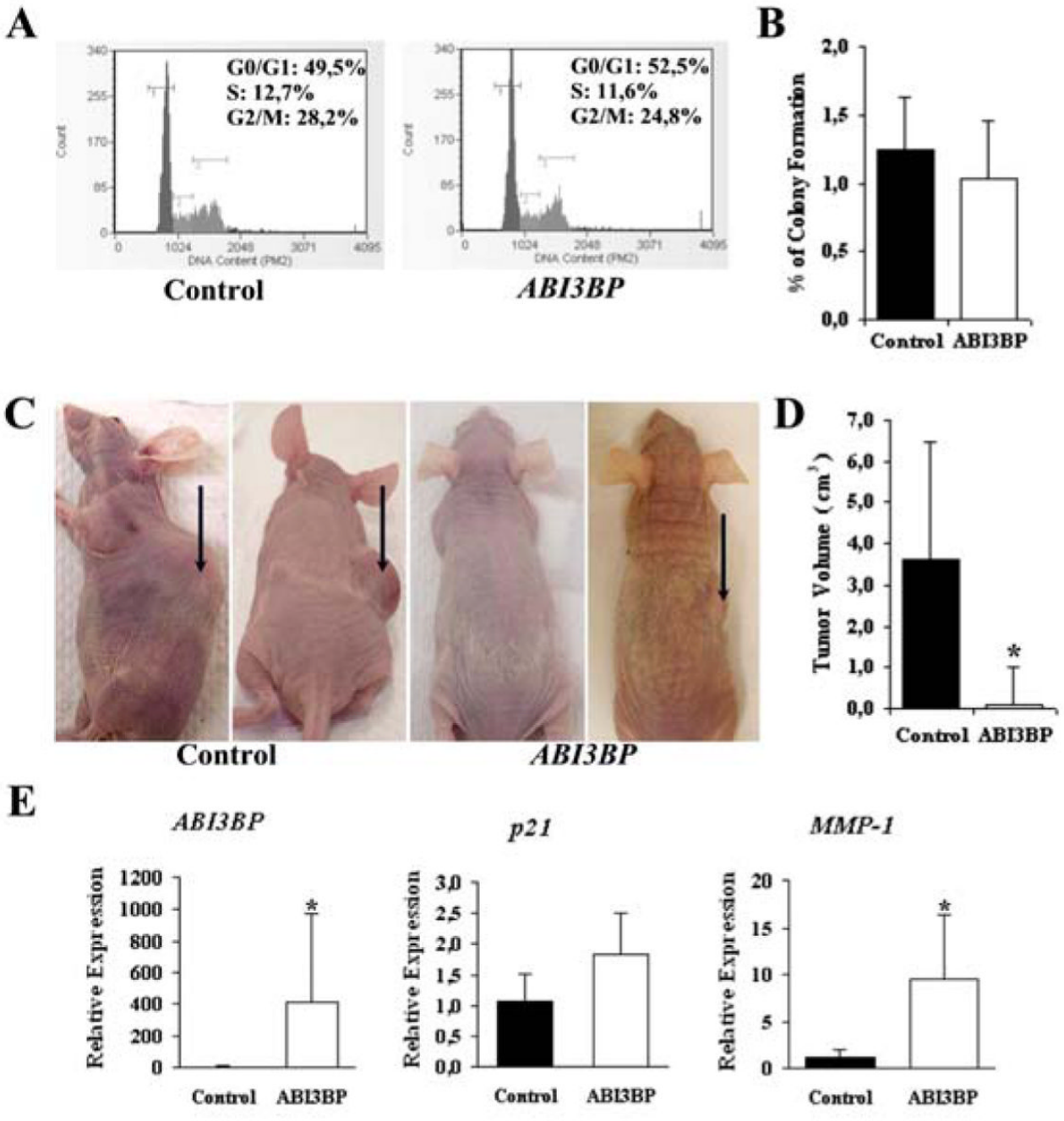

Figure 4.

Effect of *ABI3BP* re-expression in cell cycle, anchorage-independent cell growth and tumor growth in nude mice. Black bars correspond to control clones (n=2) and white bars correspond to *ABI3BP* expressing clones (n=2). In *A*, effect of *ABI3BP* expressing cells on cell cycle. The percentage of cells and cell cycle distribution is shown using Guava CytoSoft 2.1.4. Cells expressing *ABI3BP* showed a slight growth arrest when compared with control cells. In *B*, the graph shows the anchorage independent growth. Although the percentage of colony formation in soft agar is decreased in ARO cells expressing *ABI3BP* in comparison with control cells, it was not a significant increase. In *C*, representative animals that received either control cells (animals with tumor formation in the first two panels) or cells expressing *ABI3BP* (animals

with no tumor or smaller tumor in the last two panels). The arrows point to formed tumors. *D*, tumorigenicity experiments are summarized in the graph showing mean ± SD of the volume of tumors after inoculation of ARO cells. At least 6 animals were inoculated per group. In *E*, graphs show mean ± SD of *ABI3BP*, *p21* and *MMP-1* relative expressions of formed tumor of nude mice. We observe an increased *p21* and *MMP-1* expressions when *ABI3BP* was re-expressed

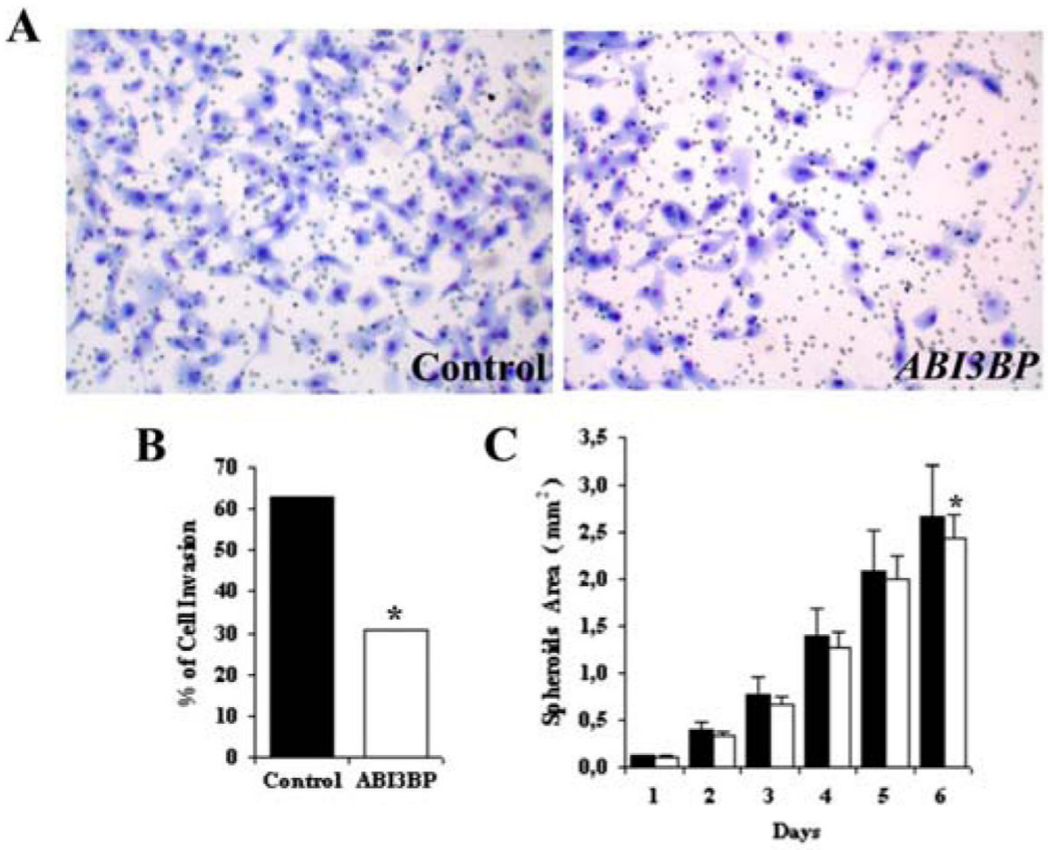

Figure 5.

The effect on invasion and migration following *ABI3BP* re-expression in the WRO cell line. Black bars correspond to control clones (n=2) and white bars correspond to *ABI3BP* expressing clones (n=2). *A*, representative results of invading cells are shown with a 100X magnification. Cells expressing *ABI3BP* decreased the percentage of invasion. *B*, the percentage of invasive cells in a Matrigel assay is shown. The mean ± SD of the percentage of triplicates are shown. *C*, cell migration was assessed by plating tumor spheroids and measuring the area covered by tumor cells migrating from the originating spheroid over time. The graphs display the mean ± SD of at least 12 spheroids of each clone. Tumor cell migration was impaired in cells expressing *ABI3BP* after the second day.